

Reaction cell for in situ soft x-ray absorption spectroscopy and resonant inelastic x-ray scattering measurements of heterogeneous catalysis up to 1 atm and 250 °C

P. T. Kristiansen, T. C. R. Rocha, A. Knop-Gericke, J. H. Guo, and L. C. Duda

Citation: [Review of Scientific Instruments](#) **84**, 113107 (2013); doi: 10.1063/1.4829630

View online: <http://dx.doi.org/10.1063/1.4829630>

View Table of Contents: <http://scitation.aip.org/content/aip/journal/rsi/84/11?ver=pdfcov>

Published by the [AIP Publishing](#)

Articles you may be interested in

[A high pressure cell for supercritical CO₂ on-line chemical reactions studied with x-ray techniques](#)
Rev. Sci. Instrum. **85**, 093905 (2014); 10.1063/1.4895717

[A setup for resonant inelastic soft x-ray scattering on liquids at free electron laser light sources](#)
Rev. Sci. Instrum. **83**, 123109 (2012); 10.1063/1.4772685

[A von Hamos x-ray spectrometer based on a segmented-type diffraction crystal for single-shot x-ray emission spectroscopy and time-resolved resonant inelastic x-ray scattering studies](#)
Rev. Sci. Instrum. **83**, 103105 (2012); 10.1063/1.4756691

[Electron-hole correlation effects in core-level spectroscopy probed by the resonant inelastic soft x-ray scattering map of C60](#)
J. Chem. Phys. **135**, 104705 (2011); 10.1063/1.3633953

[High pressure in situ x-ray absorption spectroscopy cell for studying simultaneously the liquid phase and the solid/liquid interface](#)
Rev. Sci. Instrum. **76**, 054104 (2005); 10.1063/1.1914787



Reaction cell for *in situ* soft x-ray absorption spectroscopy and resonant inelastic x-ray scattering measurements of heterogeneous catalysis up to 1 atm and 250 °C

P. T. Kristiansen,^{1,2,3} T. C. R. Rocha,² A. Knop-Gericke,² J. H. Guo,⁴ and L. C. Duda¹

¹Department of Physics and Astronomy, Division of Molecular and Condensed Matter Physics, Uppsala University, Box 516, S-751 20 Uppsala, Sweden

²Abteilung Anorganische Chemie, Fritz-Haber-Institut der Max-Planck-Gesellschaft, Faradayweg 4-6, D-14195 Berlin, Germany

³Helmholtz-Zentrum Berlin für Materialien und Energie Albert-Einstein-Str. 15, D-12489 Berlin, Germany

⁴Advanced Light Source, Lawrence Berkeley National Laboratory, Berkeley, California 94720, USA

(Received 22 September 2013; accepted 26 October 2013; published online 19 November 2013)

We present a novel *in situ* reaction cell for heterogeneous catalysis monitored *in situ* by x-ray absorption spectroscopy (XAS) and resonant inelastic x-ray scattering (RIXS). The reaction can be carried out at a total pressure up to 1 atm, a regime that has not been accessible to comparable *in situ* techniques and thus closes the pressure gap to many industrial standard conditions. Two alternate catalyst geometries were tested: (A) a thin film evaporated directly onto an x-ray transparent membrane with a flowing reaction gas mixture behind it or (B) a powder placed behind both the membrane and a gap of flowing reaction gas mixture. To illustrate the working principle and feasibility of our reaction cell setup we have chosen ethylene epoxidation over a silver catalyst as a test case. The evolution of incorporated oxygen species was monitored by total electron/fluorescence yield O K-XAS as well as O K-RIXS, which is a powerful method to separate contributions from inequivalent sites. We find that our method can reliably detect transient species that exist during catalytic reaction conditions that are hardly accessible using other spectroscopic methods. © 2013 AIP Publishing LLC. [<http://dx.doi.org/10.1063/1.4829630>]

I. INTRODUCTION

One of the main challenges for obtaining more detailed knowledge about heterogeneous catalysis is the difficult task to perform analytic measurements of the reaction process under realistic, industrially relevant, conditions. An estimated 90% of all commercial chemical products have been subject to a catalytic reaction at some point of their production.¹ Thus the contribution to the global annual gross domestic product of goods and services involving heterogeneous catalytic processes exceeds a value of USD 10 trillions.² This is one, strong motivation for developing site and species specific methods to investigate crucial stages of a given catalytic system and, ultimately, improve its performance.

Such measurements would be of great significance because certain reaction paths could be pressure dependent and not down-scalable. For instance, there is evidence³ for metastable bulk-dissolved and surface oxygen species that rapidly disappear outside these conditions in the prototypical catalytic epoxidation of ethylene over Ag.

We recall the following three steps that govern heterogeneous processes (assuming a solid metal catalyst for simplicity):

- (i) The reactant molecules impinge on the surface of the metal catalyst and may bond to the metal if the anti-bonding states are pushed above the Fermi level⁴ forming new bonding and anti-bonding states.
- (ii) The chemically adsorbed reactants, which are now bound to the catalysts surface, experience weaker inter-

nal bonds⁵ and may now more easily bond to other surface, sub-surface species or molecules in the gas phase.

- (iii) The formed reaction products may desorb from the catalysts surface.

Unravelling the complexity of step (ii) prompts the use of atomically specific techniques that allow to probe *in situ* the catalytic reaction and the changes of electronic structure. However, so far, most electronic structure studies have been performed either under UHV conditions or *ex situ*, on post-reaction surfaces. Recently, it has become possible to perform x-ray photoelectron spectroscopy measurements at reaction gas mixture pressures up to a few mbar.⁶ However, this still presents a substantial pressure gap to conditions that resemble the industrial process.

It is well-known⁷⁻⁹ that x-ray excited core-level spectroscopies, such as x-ray absorption spectroscopy (XAS) and x-ray emission spectroscopy (XES), also called resonant inelastic x-ray scattering (RIXS) when it is used resonantly, are powerful electronic structure techniques supplying complementary information about local, i.e., site specific, electronic structure. Instrumentation for XAS and RIXS normally requires a high or an ultrahigh vacuum environment. However, the use of x-rays facilitates penetration of thin silicon nitride membranes, which are strong enough to withstand the necessary pressure difference between the ambient environment of an active catalyst and the vacuum chamber.

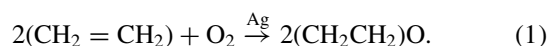
In this report, we will show how it is possible to take the advantage of these two techniques, XAS and RIXS, in the study of *in situ* heterogeneous catalysis, guided by using the

example of epoxidation of ethylene over Ag. For this purpose, we present the design of a reaction cell for heterogeneous catalysis and report on its functionality when probing with synchrotron radiation based XAS and RIXS. We also show how the cell can easily be adapted to investigate similar types of reactions, including even UV-activated catalysis as well as electrochemical reactions at solid/liquid interfaces.

The rest of the article is organized as follows: first, we present a short introduction to the catalytic reaction that we use as a test case for the reaction cell (Sec. II). Then, we describe in detail the construction of our reaction cell platform (Sec. III). In Secs. IV and V, we report results of operation of the cell using a thin film and a powder catalyst, respectively. Sec. VI gives an account of first results from *in situ* x-ray spectroscopy experiments using our reaction cell. Section VII contains a brief summary of modifications to the reaction cell design in order to adapt to needs for monitoring photochemical and electrochemical reactions, respectively.

II. EPOXIDATION OF ETHYLENE OVER AG

Ethylene oxide (EO) is an example of a catalytically obtained chemical of major importance. For instance, in the year 2008, 52 major market participants¹⁰ combined for an annual production of EO in excess of 19 Mt, making EO the 14th most-produced organic chemical¹¹ in the world. Modern commercial synthesis of EO is based on partial oxidation of ethylene over a heated ($>180^{\circ}\text{C}$), silver-based catalyst at total pressures in the order of 10 atm. Over the last 30 years much effort has been made to improve the level of knowledge for optimizing the exploitation of this process.¹² A simplified reaction scheme can be written as



However, in detail, the reaction mechanism involves a variety of oxygen species that reside on/in the silver surface and bulk, the roles of which are still insufficiently well understood to account for the reaction pathway on the atomic scale.¹³

We have chosen to investigate ethylene epoxidation by Ag as a first test for our novel platform, first, because it is an important system not only commercially but due to fundamental considerations.¹⁴ Second, this system presents particular technical challenges, such as distinguishing between contributions from several different oxygen species in Ag, as well as in the gas phase (gaseous O_2). Several oxygen species have been identified in previous *ex situ* studies and a model was proposed,^{15–17} in which the active sites consist of two oxygen species, one nucleophilic and the other electrophilic. In particular for high pressure and/or high temperature reactions, such a reaction scheme suggests that the active sites are metastable and may only exist during reaction.³ The characteristics of x-ray spectroscopy as a core level spectroscopy provide a powerful way to monitor the evolution of different oxygen species in and on the catalyst material. Moreover, the development of suitable *in situ* and *in operando*¹⁸ platforms, allowing to monitor reactions in real time, are needed to obtain reliable information of the actual reaction paths, which

can give feedback in order to improve existing schemes for heterogeneous catalysis.

III. DESIGN OF THE REACTION CELL PLATFORM

A. Overview

Sections III B–III E outline the working principle of the cell when it is used to investigate oxygen species during ethylene epoxidation over Ag. It also serves as a more general description, as many features are common to the design for UV-activated or electrochemically driven reactions, see Sec. VII for these alternatives.

In order to achieve the desired *in situ* XAS and RIXS capability we strived to fulfill the following conditions: (i) The conditions under which the reaction occurs must mimic industry parameters. (ii) The product yield of the reactions must be sufficiently large for a reliable detection in flow mode, i.e., the gas analysis is performed in real time. (iii) Moreover, in order to perform soft x-ray measurements, the setup must be UHV compatible.

Our experimental setup can be broken down into the following essential parts:

- X-ray source from a modern synchrotron radiation source.
- XAS and RIXS detector systems.
- Vacuum compatible reaction cell system.

In order to perform any x-ray spectroscopy with the cell, a synchrotron undulator radiation source is needed and the used beamline should be optimized for performing soft x-ray RIXS measurements. This means that the available flux should be no less than 10^{12} photons/(s \cdot 0.1% bandwidth) and that the resolving power $E/\Delta E$ should exceed 5000. The presented results have been obtained at beamline 7.0.1 at the Advanced Light Source, ALS, in Berkeley, CA and beamline U41-PGM¹⁹ at BESSY in Berlin. At both stations, we have used a home laboratory built Nordgren-type²⁰ RIXS spectrometer, now also commercially available by Scienta²¹ under the product name *Scienta XES350*.

By exciting the sample with soft x-rays it is possible to obtain chemically selective information of both the unoccupied states, using XAS, as well as the occupied states, using RIXS. The total fluorescence yield (TFY) emitted from the sample is recorded by using a photodiode or channeltron and it is a measure for the absorption coefficient in the bulk. The total electron yield (TEY) is obtained by measuring the sample drain current and it reflects the absorption coefficient close to the surface. In this work, we typically scan the monochromator energy in the range 510–570 eV to obtain oxygen K-edge XAS. In RIXS, the sample is excited resonantly at an absorption edge feature (within several eV of the threshold), corresponding to an empty orbital. A bound state is created, which decays on a femtosecond time scale by emission of a new photon. The spectrum of these scattered photons is recorded, which reflects the low-energy excitations (up to several eV) and serves as a fingerprint for each species. The RIXS spectrometer used for this work has been previously described in detail in Ref. 20. Several synchrotron radiation

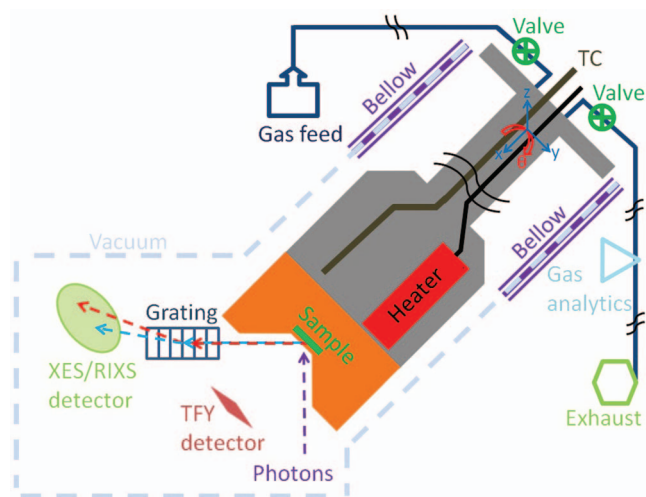


FIG. 1. Schematic principle diagram of our cell system (not to scale). This includes the gas feed system (top), the rod inserted into the endstation (outlined by the dashed line), gas analysis instrumentation (triangle on the right), security solenoid valves (crossed circles), and thermocouples (labeled TC). The catalytic reaction cell holding the catalyst material (green square) is placed in the beam focus. The purple arrow indicates the incident x-ray beam entering the cell and the re-emitted photons that are analyzed by a grazing incidence x-ray spectrometer. A photo diode or a channeltron serve as the TFY detector (the rhombus). TEY is measured by measuring the sample current using a thin wire to the catalyst material (not shown).

facilities and their beamlines^{19,22,23} have been used as x-ray sources in the present work.

Before we describe the results of our *in situ* x-ray spectroscopy (Sec. VI), Secs. III A–III E are concerned with the description of the novel reaction cell constituents that we have designed and constructed. The *reaction cell system* (Fig. 1), which is inserted into a vacuum chamber for x-ray spectroscopy measurements, can be broken further down into the following parts:

- *Gas feed system* that transports and mixes the gaseous reactants.
- *Sample holder and in vacuo manipulation*.
- *Catalytic reaction cell head* where the catalysis takes place and can be monitored by XAS/RIXS.
- *Gas analysis instruments* such as a quadrupole mass spectrometer and/or gas chromatography to analyze the gaseous reaction products.

Gas tubes (blue lines in Fig. 1) that connect the gas manifold to the cell are fitted with commercial interlock solenoid safety valves (DYNAMCO). These have electromagnetic actuators that quickly close the valves should the pressure in the end station exceed the chosen set point. In case of membrane failure, the gas volume inadvertently introduced to the end station will then amount to no more than ~ 5 ccm, which has been found to produce a peak pressure of less than 10^{-3} mbar before the gas can be pumped away again.

In order to monitor the catalytic activity, the reaction gas products that leave the cell are led to gas analysis instruments. The gas analysis consists of one or more of the following instruments: a quadrupole mass spectrometer (QMS 200 M with C-SEM, Pfeiffer Vacuum), a gas chromatograph (CP-4900

Micro-GC, Varian), or a proton-transfer-reaction mass spectrometer (not available to us). The latter two instruments are best for the ethylene epoxidation process, because the mass of EO coincides with that of CO_2 and thus produce overlapping QMS signals. However, due to the occurrence of characteristic satellite mass peaks (fractured molecules) a sufficiently sensitive QMS can still be used to distinguish between the concentration of these two species.

The vacuum parts of the reaction cell system (grey and orange areas in Fig. 1) consists of two pieces, a retractable hollow rod and the cell head, which are screwed together, by M26 threads, and sealed vacuum tight by an Viton o-ring. The rod is a tube, open to the ambient atmosphere, that is welded to a Conflat® 64 flange (grey area in Fig. 1). This solution is convenient if adaptation to different geometries, e.g., at different endstations, is required, because only the length of the rod and the tubes leading to the cell need to be changed.

The reaction cell head is made of a stainless steel cylinder with a circular cross section of 3 cm diameter and a length of 7 cm and attached to the rod, as guided by previous experience.⁹ This platform is inserted into an existing end station where it can be manipulated in x -, y -, z -, and θ -direction. This way, the sample area to be probed can easily be placed and manipulated in the focal spot of the synchrotron radiation beam by a manipulator (Fig. 1).

B. Catalyst material and geometry

Recalling the issue of separating oxygen signals originating from species within the catalyst material and the molecular oxygen in the reaction gas mixture, we have experimented with two different approaches, namely:

- evaporating a thin film of the catalytic material directly onto the a Si_3N_4 membrane (Fig. 2(a)).
- placing bulk material of the catalyst (e.g., powder) closely behind the membrane (Fig. 2(b)) fixed by a clamp (Fig. 2(c)).

A thin film offers the possibility to control the thickness of a catalyst material that the x-rays penetrate before entering the gas reaction mixture. This allows one to vary the ratio between contributions from oxygen species in Ag on the one hand and the background gas phase contribution to the total spectroscopic signal on the other hand. Moreover, finite size effects may be studied. The alternative is to fit the cell with a pellet of compressed (Ag) powder. This is advantageous for instance in case the reaction on a thin film does not yield a sufficient concentration of the reaction product (i.e., ethylene oxide) or if one, for instance, wishes to study an alloy catalyst that may be difficult to evaporate onto the membrane in a controllable way. Also in this case the choice of different grain sizes (e.g., nano-powder²⁴) provides the option to study finite size effects.

1. Thin film catalyst

In this configuration, a thin film of Ag (thicknesses in the range 14–68 nm were tested) is deposited by resistive

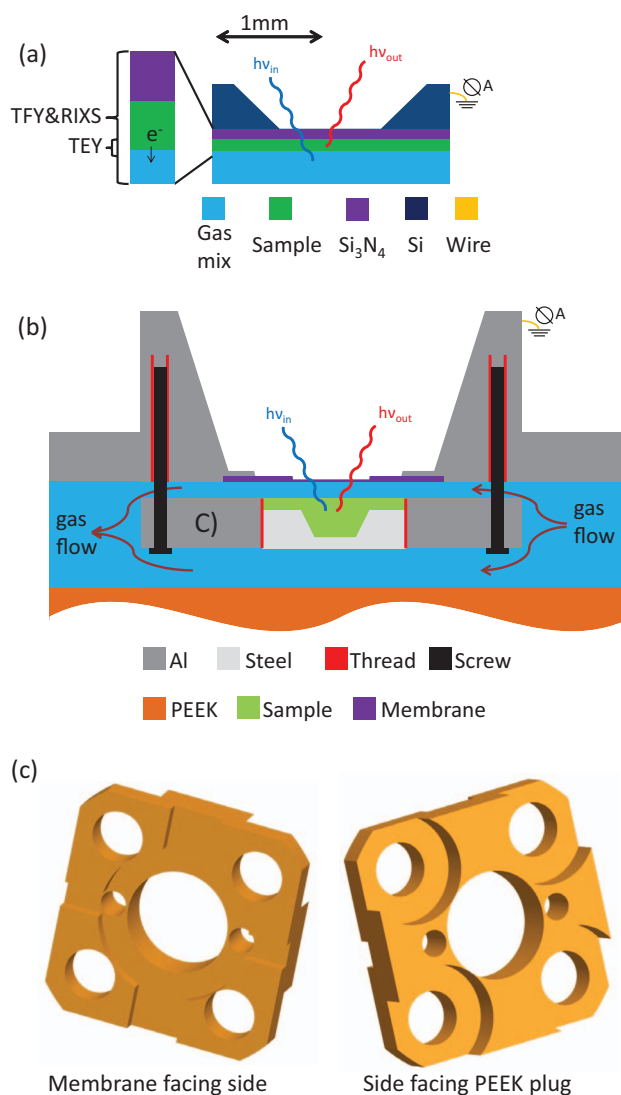


FIG. 2. Schematic diagram (roughly to scale) of the cell parts close to the sample in configuration in the film-, (a), and powder-configuration, (b). The different probing depths/methods are indicated. (c) is 3D tilted views of the of the clamp that is screwed into the membrane cap, by the four outermost holes. The powder sample holder is screwed (threads not shown) into the center of the clamp. Grooves on the membrane-facing side and around the threaded sample holder have been milled away to increase the gas flow to the sampling area of the powder.

evaporation onto a thin, x-ray transparent membrane (green area in Fig. 2(a)). The x-rays penetrate the membrane material from the top of the figure and proceed through the Ag-film and finally reach the gas mixture (blue area in Fig. 2(a)).

The x-ray window membrane is a commercially available²⁵ thin film of silicon nitride on a silicon wafer frame of $5 \times 5 \text{ mm}^2$ area and $200 \mu\text{m}$ thickness. The membrane area was chosen to be $1.0 \times 0.5 \text{ mm}$ and the membrane thickness is 100 nm . These dimensions have been found to be appropriate to ensure that the membrane stays intact for the entire duration of the *in situ* x-ray spectroscopy and withstands stress from pressure differences, heating, and x-ray irradiation. The silicon frame is attached to a metal supporting disk by a silver-based adhesive epoxy glue (EPO-TEK[®] H21D²⁶) that creates a vacuum tight seal, see Fig. 3. The epoxy is electrically conductive and in contact with the deposited Ag film, allowing



FIG. 3. Photos of the disassembled reaction cell. (Top) Picture of the front end of the cell with the PEEK cap removed. (a) Tightening cap (PEEK) with viton rings for sealing. (b) the reaction cell body with hole in its top end for differential pumping. (c) is the membrane holding cap that can be “sandwiched” between the two small viton rings. The threaded top hole is to fasten the TEY cable. (Bottom) (a) part the rod that connects to the back side of the cell seen in (b) with its various connection holes. (c) is the membrane holder with the internal surface facing the camera.

the sample current to be measured by a signal cable (yellow line in the top part of Fig. 2) that is screwed (not shown) to the holder disk and goes on the outside of the rod to an electrical vacuum feed through. The TFY and RIXS signals are detected by x-rays that are re-emitted through the membrane.

NB: In this configuration, the cell can also be easily adapted for studying *in situ* electrochemical reactions, e.g., water splitting or UV activated samples (see Sec. VII).

2. Powder catalyst

In this configuration, the sample is a compressed powder (green area in Fig. 2(b)), an uncoated Si_3N_4 membrane is used (purple area in Fig. 2(b)), and the metal disk holding the membrane is modified as shown (grey area in Fig. 2(b)). The x-rays first penetrate the Si_3N_4 , then the gap filled with the gas mixture, and finally the active catalyst material. The gas-filled gap must not exceed some tens of μm , so that a minimum of photons be absorbed by the gas mixture and lost for generating the desired spectroscopic signal. On the other hand, the gap must still be kept sufficiently large to ensure that the catalytic reaction not be kinetically restricted. Moreover, to avoid excessive pressure on the membrane, the cell

geometry features a bypass channel through which most of the gas is allowed to flow. Although we have not pursued this further, it could be desirable to either omit the bypass, e.g., using a gas feed system including mass flow meters that can supply/control sufficiently small gas flows. Alternatively, one could incorporate a gas sniffer in the downstream of the sample in the gap. Both of these cell modifications avoid diluting the gaseous reaction products with the reaction gas mixture and hence probably improve the gas analysis and conversion rate measurements (see below).

In the Ag powder experiments presented below, we have avoided the kinetically limited regime by considering the following: Balzhinimaev²⁷ reports that a Ag powder with an average grain size of 2 μm diameter consumes about 10^{18} molecules of ethylene $[(\text{m}^2 \text{Ag})^{-1} \text{s}^{-1}]$ in the production of ethylene oxide with a selectivity of about 50%. Thus, we estimate that it is sufficient if twice of the latter amount is supplied to the Ag powder in order to stay away from the kinetic limit. There is about 10 mg of active powder with an estimated average particle diameter smaller 2 μm (which is less reactive than the 2 μm powder²⁷), amounting to a total active surface area of $28 \times 10^{-4} \text{m}^2$. This implies that 5.7×10^{15} molecules of ethylene per second should be exchanged in the reaction volume. At a total flow of 2.5 SCCM of ethylene and a bypass (see above and Fig. 2) of 95%, the flow of ethylene molecules across the powder equals about 5.3×10^{15} per second, i.e., roughly the required flow.

C. The catalytic reaction cell

Fig. 3 shows photographs of the disassembled reaction cell. The top photo shows (a) the tightening cap, (b) the cell body with the front part facing the camera, and (c) the membrane holder as used in setup B (for powder samples). The membrane holder has groves milled into it to allow photons to enter and leave the membrane area. The path of incident and emitted x-rays is indicated with a purple and blue arrow, respectively.

The bottom photo of Fig. 3 shows (a) part of the rod with (d) gas feed lines (two are for the gas flow and one is for the differential pumping), and (e) the heating cartridge, which has a thermocouple at its center. (b) is the cell body with the back part facing towards the camera with the connection holes visible, and (c) is the membrane holding disk as used in setup A. The actual membrane size is evident by the small light area at the center of the disk piece and part of the Si_3N_4 membrane is left free (the blue triangle area, indicated with a red arrow) to enable stylus profilometer measurements of the film thickness. Not shown are two thermocouples going into the two smaller holes of the cell. Note the two black viton gaskets, which are there to enable a differential pumping of the threaded volume. The threads appear dark due to the heat resistant grease applied.

Figure 4 shows a principle drawing cross section through a plane parallel to the cylindrical axis of the cell head, which is screwed onto the rod. Vacuum-tight sealing between the rod and the cell head is achieved by two Viton O-rings (bottom four black circles in Fig. 4) one at the beginning of the

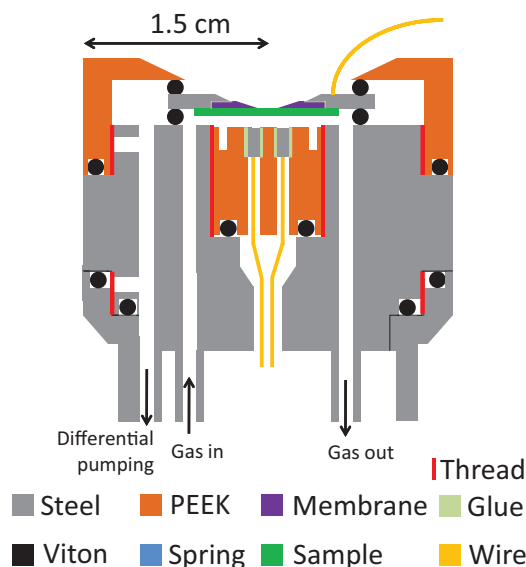


FIG. 4. Cross section of the catalytic *in situ* cell. Here, the cell is shown in its configuration (A), where the catalytic material (green) is evaporated directly onto the membrane, which also serves as a gas-vacuum barrier. The outer diameter of the cell is 3 cm.

thread (red lines in Fig. 4) and one at the end, see Fig. 3. The volume between the two Viton gaskets is kept at a pressure of a few mbar by a membrane pump that is connected by thin tubes and channels drilled into the body of the cell (Fig. 4 marked as “differential”). The differential pumping improves vacuum conditions in the surrounding UHV chamber, which has proven to be necessary when heating the cell to temperatures above the catalytic reaction point for ethylene epoxidation at 180 °C. The vacuum seals at the membrane-end of the cell (top four black circles in Fig. 4) are also differentially pumped by the same channel system.

The bulk of the cell head is made of stainless steel which can be heated by a cartridge²⁸ to a constant and uniform temperature. The heater is shown in Fig. 1 as is one of three thermocouples. This ensures that both the catalytically material and the inflowing reaction gas mixture attain the same desired temperature via heat conduction. The gas inlet is shown on the bottom left and the gas is directed via a drilled channel to the reaction volume at the top center of the figure. The tubes that transport the gas are attached to the cell by soldering onto standard stainless screws that have been drilled out through the center and screwed into threaded holes in the cell head. These connections are sealed by Viton O-rings that are fitted in tapered grooves that retain the O-rings upon tightening.

A screw cap (top part of Fig. 4 in orange) made of PEEK (polyether ether ketone) serves as a clamp that compresses the Viton O-rings (top six black circles in Fig. 4) to achieve a vacuum-tight sealing between the cap and the metal disk holding the membrane, and also between the reaction gas and the roughly pumped channels. This cap setup allows for an easy exchange of the x-ray window membrane assembly and switching between different catalyst geometries (see Sec. III D).

The reaction gas mixture in the reaction volume close to the catalyst is separated from the UHV by a 100 nm Si_3N_4

thick x-ray membrane (purple area in Fig. 4). The Si frame holding the membrane is glued onto a disc-shaped holder and “sandwiched” between a pair of o-rings, held in place by the force of the PEEK cap. Additional differential pumping of the dead volume between the o-rings (white areas in Fig. 4) prevents excessive outgassing when the cell head is heated.

D. Vacuum sealed parts

The central plug in setup (A) (square orange area Fig. 4) is made of a threaded PEEK piece that seals the reaction cell from the ambient atmosphere by a Viton O-ring. The two electrodes are sealed by a drop of glue (EPO-TEK® H21D²⁶) applied to the top part of the thread of the PEEK plug. Metal electrodes, with wires soldered onto them, are screwed in from the top side. These electrodes serve as sensors (by reading their drain current) to assure that the cell has been correctly placed in the synchrotron beam and that the x-rays are entering the cell.

A PEEK plug can also be used when applying alternative setup (B). In this geometry, one should minimize the size of the gap between the membrane and the sample in order to avoid excessive absorption of the x-rays by the gas mixture. On the other hand, such a narrow channel could lead to a pressure build-up on the membrane, exceeding the breaking limit of about 1.3 atm unless a much-reduced flow is used, requiring controllers to accuracies better than about 0.1 SCCM and correspondingly low leak rates. Instead, we have introduced a bypass channel between the back side of the sample holder and the PEEK plug. When allowing for such a bypass, one always needs to ensure that the catalytic reaction does not become kinetically limited and thereby lead to artificial conditions. The bypass ratio can be controlled by altering the gap between the PEEK plug and the backside of the powder sample holder, Fig. 2(c), by altering the length of the PEEK plug. The particular reaction to be investigated will determine the details of the geometry. In any case, such an arrangement leads to more diluted reaction products in the outlet gas and thus makes their detection more challenging but still feasible.

E. Catalyst temperature control

Figs. 1 and 3 also document the option to heat the cell above room temperature. Temperature control is achieved by a commercially available²⁹ high density cartridge (230 V max 150 W, Ø6.5 × 50 mm) fitted in a hole drilled 6 mm off center of the rod axis. A J-type thermocouple is built in at the center of the cartridge, allowing to read its local temperature which is useful during ramping. Apart from the internal thermocouple of the cartridge, there are two holes drilled from the back side of the cell that can accommodate a thermocouple each. One hole is shallow, approximately 1 cm, and the other is as deep as possible, approximately 6 cm, allowing to check the uniformity of the heating. Our experience has shown that the three thermocouples readings stay within 4 °C of each other, once the cell has reached a stabilized temperature.

At least 40 min should be allowed for elevating the temperature of the entire cell head, when situated in vacuum and

fitted with a membrane, from room temperature to 180 °C. The reason for this is that, in our experience, one must keep the heating rate below 4 °C/min to avoid that the membrane ruptures due to any excessive temperature gradient. Note also that it is preferable to use a channeltron to obtain the TFY signal when using the cell at elevated temperatures (Fig. 1) since photodiode readings tend to be very sensitive to heat gradients over their active area.

The reaction gas mixture reaches the catalytic surface via drilled channels (3 mm diameter, 70 mm total length). At the typical total flow rate of 5 sccm, the power needed to heat it is less than 1 W, a rate that leads to thermal equilibrium between the walls and the gas already within a few millimeters of tube length.

IV. OPERATION WITH THIN FILM CATALYST

The film can be deposited, e.g., by resistive heating evaporation of the catalyst material *ex situ* in a separate vacuum chamber. When evaporating Ag we have used a tungsten “boat” coated with Al₂O₃. The sample thickness is monitored by a calibrated quartz crystal microbalance during deposition and measured with a stylus profiler afterwards. We have used thicknesses in the range of about 10–70 nm. The thickness must be optimized by considering the penetration depth³⁰ of the incident and scattered x-rays, as well as by taking into account any structural changes of the film during operation. The latter is observed for instance during ethylene epoxidation where the thin Ag film tends to form islands.

Prior to exposure, the film yielded a completely structureless scanning electron micrograph (SEM). Fig. 5 shows a SEM of a Ag thin film sample after exposure to reaction conditions and beam. Note that the membrane in area C is missing (thus the black color). This is hardly avoidable because the membrane with the exposed film becomes brittle after

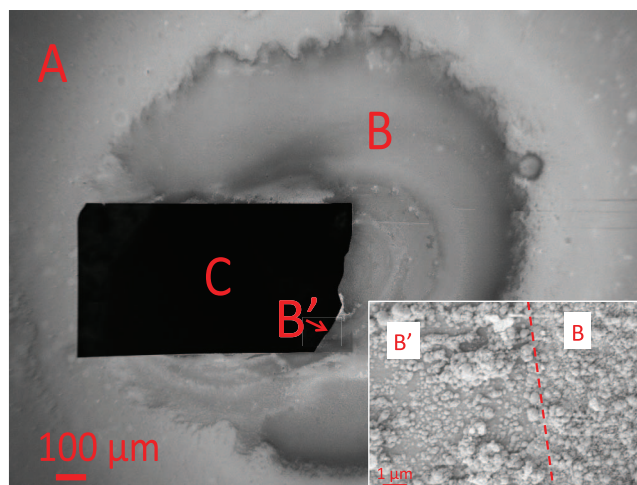


FIG. 5. Scanning electron micrograph (SEM) of a uniformly 31 nm thick Ag film that has been applied for ethylene epoxidation at $T = 225\text{ }^{\circ}\text{C}$. Areas A, B, and B' show different morphologies of the exposed Ag film. Area C is where the membrane has disappeared due to post-reaction rupturing. The lower right corner of the rectangular membrane is still attached to the frame and marked (arrow) as area B'. (Inset) Zoom of the areas B' and B, where the membrane meets (at the dashed line) the supporting Si.

exposure and easily ruptures when being retrieved from vacuum. In the outermost area A of the SEM-picture the sample is still film-like to the eye but it is significantly less shiny (it looks white and dull) than a pristine Ag film, probably due to strong oxidation. In the roughly circular-shaped area B, the Si_3N_4 is found to be partly exposed and the Ag film has largely undergone a transformation into islands of Ag crystals.

The inset of Fig. 5 shows that island formation is more pronounced on the membrane than on the supported Si_3N_4 , presumably due to a higher temperature on the membrane since excess heat from the chemical reactions and the beam is accumulated due to the low heat conductivity of the thin membrane. Note also the pronounced asymmetry of the film morphology (area B) with respect to the membrane center, matching the direction of the gas that was from left to right in the SEM. This suggests that the membrane area was hotter than the surroundings and excess heat has been transported by the gas to other areas of the film (“hot gas plume”) thus causing the asymmetric appearance around the membrane. The heat conduction on the Si_3N_4 membrane, 30 W/(m K), is much lower than that of the Si frame, 149 W/(m K), leading to a higher local temperature. Heat is produced in large part by the exothermic chemical reactions, i.e., 25 kcal/mol due to the epoxidation process and 340 kcal/mol from total combustion, plus any additional beam heating. Apart from the local temperature where x-rays probe the film being somewhat higher than the rest of the film, this probably does not lead to a substantial deviation from industrial conditions to the extent of causing artifacts. Since Ag has a much higher heat conductivity than Si, 429 W/(m K), using a thicker film could be used to reduce the membrane heating, if desired. Moreover, the observation of a “hot gas plume” suggests that heat dissipation from the membrane also could be increased by diluting the reaction mixture with He, which has a high thermal conductivity, 0.15 W/(m K), which, for instance, is about nine times higher than that of Ar (see below).

In the Ag film experiments discussed below, we always strived to maximize signals from the Ag material by translating the sample in the beam to find spots that yielded a small molecular oxygen contribution.

V. OPERATION WITH POWDER CATALYST

Fig. 6 displays a SEM of a post-reaction Ag powder sample. The initial sample preparation is as follows: First, the powder is pressed into the sample holder by sliding the sample holder into a hollow tube with a tight fit. Next, the sample powder is filled into the hollow rod and finally compressed using a tight fitting rod. It is advantageous to use a flat ended rod to compress the powder and form the sample holder as shown in Fig. 2, with a shallow outer rim and a deeper central part. This will lead to a strongly compressed sample at the outer rim (D in Fig. 6) that serves to keep the more lightly compressed parts of the sample in the center (E in Fig. 6) from falling apart. Additionally, roughening the surface of the outer rim of the sample holder helps adhesion of the sample to the holder. Excess material at the sample periphery (C in Fig. 6) may easily accumulate and needs to be removed in order to

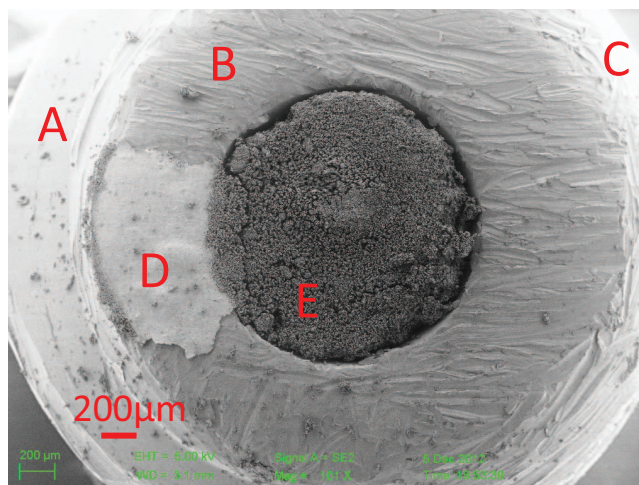


FIG. 6. SEM showing an overview of a post-reaction powder Ag sample. The letters indicate the following: thread of sample holder (A), surface area of sample holder roughened with a crude abrasive paper (B), file rounded edge (C), strongly compressed powder sample part (D), lightly compressed powder sample part (E). Note that most of the sample at the rim (D) is missing due to it falling off when retrieving it for the SEM picture after the experiments.

screw the sample holder into the clamp (Fig. 2(c)) without cracking the hard, compressed portion of the powder. Rounding the edges of the sample holder makes it easier to remove such material. The slightly lighter and apparently more dense center area of E in Fig. 6 is where the Si_3N_4 membrane was located during reaction and the x-ray measurements.

A possible way of increasing the gas flow to the sample (and thereby minimizing the bypass) could be to use a compression rod that has a hollow (instead of a flat) end with the shape of a rectangularly based frustum, matching the membrane dimensions.

Section IV has the clear advantage that the photons do not pass through the reaction mixture first. However, depending on the investigated reaction, a film catalyst may not give a sufficient yield to uniquely detect the products by quadrupole mass spectrometry or gas chromatography. In many cases the reaction in Sec. V can give a sufficient yield to facilitate detection of gaseous reaction products. However, one must be wary of undesired background signals from the gas phase in XAS using the TFY mode that is sensitive to the entire volume of the penetrated by the x-rays. In the present case, we have both gaseous molecular O_2 and oxygen species in the solid. Fig. 7 shows XAS measurements on Ag powder in an atmosphere of pure Ar and O_2 , 20 min after the measurement done in Ar atmosphere. The TEY mode is compared to the TFY mode results. The TFY shows the expected background features of gaseous O_2 spectra, i.e., the strong σ^* peak at 531.1 eV and a dip-peak-dip structure above 539.7 eV. By contrast, these features are not discernible for the TEY counterpart because only the solid sample signal is probed when measuring the drain current. Note that the pre-edge dip around 529.6 eV is a spurious signal which is due to oxide contamination on the beamline I_0 , as confirmed by the oxide peak in the I_0 -signal, that the XAS measurements are normalized with.

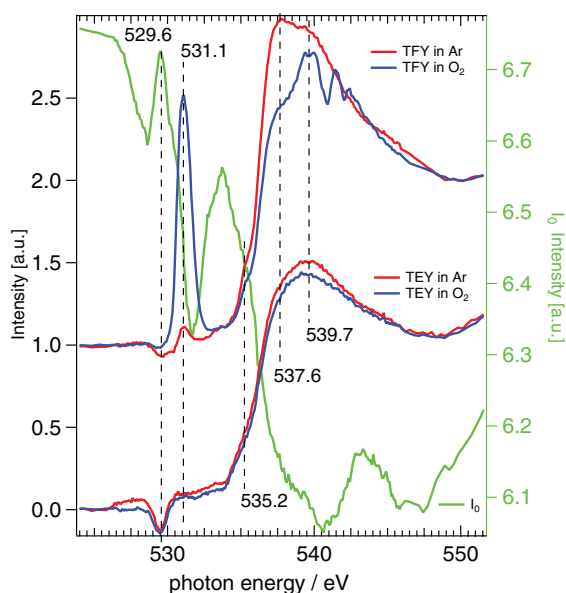


FIG. 7. XAS measurements on an Ag powder sample in Ar (red trace) and O₂ (blue trace), respectively. The shown I₀ signal with its structures is representative for both gas feeds.

VI. DEMONSTRATION OF *IN SITU* MONITORING OF ETHYLENE EPOXIDATION AT 1 ATM

The following is to demonstrate the capabilities of performing *in situ* soft x-ray spectroscopy when the cell is at ambient pressures and elevated temperatures, again, using the example of ethylene epoxidation over pure Ag at a total pressure of 1 atm and a temperature of $\sim 225^\circ\text{C}$. The presented data are accumulated on two separate measurement occasions performed at the, now decommissioned, beam line 7.0.1 at the ALS.²² Ag powder and a 31 nm thick Ag film were used at different occasions (see Sec. III A). For the Ag film the online gas analysis equipment consisted of a quadrupole mass spectrometer (QMS 200 M with C-SEM, Pfeiffer Vacuum) and for the powder the online gas analysis were both a QMS and a gas chromatograph (CP-4900 Micro-GC, Varian).

A typical experimental procedure to study ethylene epoxidation over a thin film Ag catalyst was as follows:

- A thin film of Ag is deposited onto a SiN membrane, inserted into the reaction cell system (see above), and attached to the synchrotron radiation end station.
- “Oxygen loading” procedure: the Ag film in the cell is heated to $\sim 225^\circ\text{C}$ in a pure 10 SCCM O₂ flow. These conditions are kept constant for several hours (at least 12 h) to allow the system to reach equilibrium.
- X-ray spectroscopy is performed at this stage.
- Reaction conditions: the temperature is kept constant at 225°C , while the gas feed is changed to a reaction mixture, e.g., 5:5 SCCM (O₂:C₂H₄). X-ray spectroscopy is performed during the transition and when equilibrium is reached.
- Further changes to the mixing ratio of the gases are monitored by x-ray spectroscopy similarly as described in the above procedure.

- Gas analysis of the reaction cell outlet is performed continuously to monitor the catalytic activity of the cell.

We monitored the catalytic conversion activity, as well as the selectivity towards the competing reaction products, by using a QMS and a GC. In the case of ethylene epoxidation over Ag the m/Q-ratio of the reaction products (CO₂ and C₂H₄O, respectively) from the two main reaction pathways are identical. Although this makes QMS-monitoring more challenging, the differences in the fragmentation patterns of CO₂ and C₂H₄O still makes it feasible to use this as a fast, simple, and relatively cheap solution for semi-quantitative monitoring. Note that, in particular, changes of the oxygen partial pressure causes changes of the filament burning rate leading to sensitivity changes of the QMS³¹ for masses of low partial pressures. We were able to detect an EO concentration on the level of about 4.6 ppm (500 ppm) when using Ag films (Ag powder). In the present case, the QMS also served as an indicator of the inlet gas mixture ratio because most of the inlet gas never undergoes a catalytic reaction.

An alternative is the use of a GC, which relies on the differences in retention time (which is a factor of 7 longer for EO than CO₂) of the gases in long capillary. Considering the typically low conversion concentrations of the reaction products at the cell outlet, the much increased sensitivity of the GC is a clear advantage over a QMS. A drawback for use in real time monitoring is the relatively long acquisition time of the GC, which was about 7 min in the present case.

In order to exclude artifacts and confirm that the Ag catalyst material is the cause of the conversion, we also performed several (off line) null-tests with the reaction cell over extended time periods, +24 h, without Ag catalyst material. The gas analysis then did not show any oxidation or epoxidation products when entering the reaction condition regime.

A. *In situ* x-ray spectroscopy

The evolution of the O K-edge absorption signal from the 31 nm thick Ag film during a gas feed composition change is presented in Fig. 8, where we follow the transition from a pure oxygen atmosphere (at $t < 0$ min.) to a reaction mixture of ethylene and oxygen (at $t > 0$ min). The top panel shows surface sensitive TEY mode XAS and the bottom panel shows bulk sensitive TFY mode XAS. There are two energy regions of interest: one around 531 eV with sharper structures and a main multiple peak structure starting around 535 and ending at 546 eV. Gaseous oxygen contributes structures in both regions and thus heavily overlaps with the absorbed oxygen species in the Ag film. A detailed analysis of the heterogeneous catalysis processes will be presented in Ref. 32, in the following we focus on the relevant technical aspects.

One of the main goals of using simultaneous recording of TEY- and TFY-mode data is to be able to distinguish between species residing mainly in the surface layers of the Ag film (TEY) and in the bulk of the Ag material (TFY). Studies on *ex situ*³³ Ag catalyst material as well as *in situ* measurements¹³ (at few mbar total pressure) have shown that several oxygen species are formed in/on Ag when it is exposed to gaseous O₂

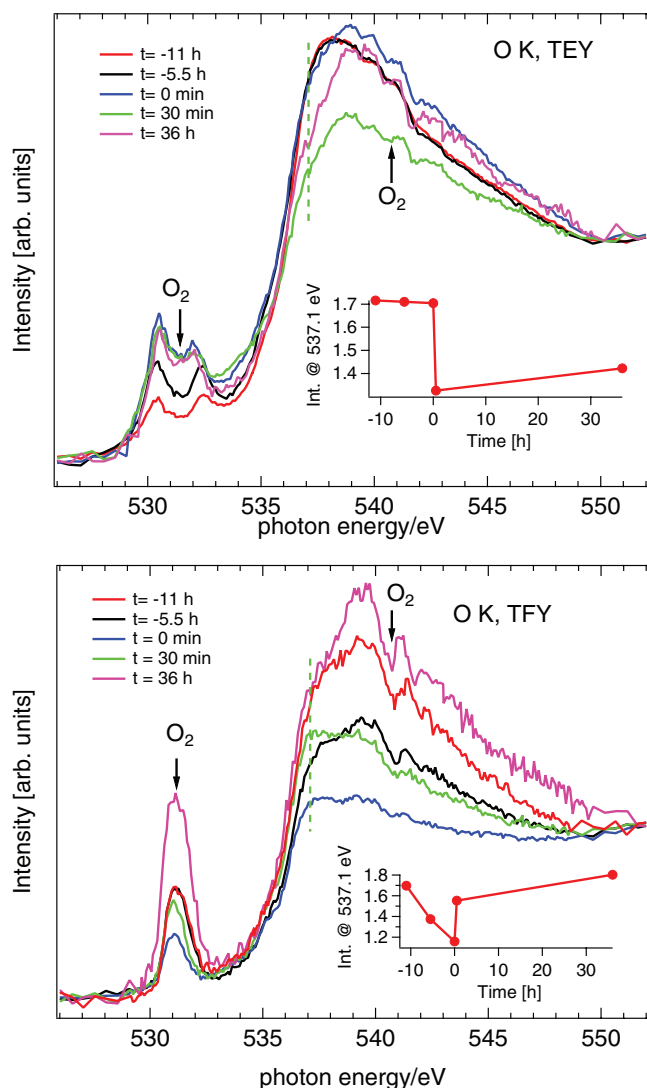


FIG. 8. XAS O K spectra of the catalytically active, 31 nm thick Ag film during gas feed composition change. Time $t = 0$ corresponds to the time of the gas change. For $t < 0$, the gas feed is pure O_2 and for $t > 0$ the gas feed is a 1:1 reaction mixture. The temperature was constant at about 225 °C.

at elevated temperatures (> 150 °C). Expectedly we observe, for instance, that bulk and surface species in this 31 nm thick Ag film have somewhat different evolutions in the observed time frame. While the main peak intensity of the bulk-like species, at 537.1 eV, immediately drops and then develops a shoulder at $t = 30$ min, the main peak intensity of the surface species shows a slower reaction and the spectrum does not change much in shape. Note that the gaseous O_2 contribution at this energy is very small (black trace in Fig. 9).

Now we turn to the low energy structure around 531 eV seen in the TEY-mode XAS. Since TEY measures the drain current from the solid with an information depth of about 5 nm,³⁴ we attribute this peak to adsorbed oxygen in the first few surface layers of the Ag catalyst (see also Fig. 2). However, we observe that the peak has a varying yet substantial “dip” that is marked “ O_2 ” as well as with a vertical dashed line. This signature, as well as weak structures at about 541 eV, probably arises from electrons produced in the gas

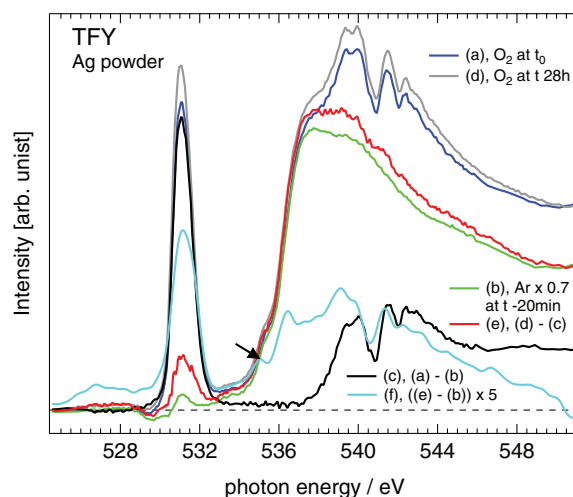


FIG. 9. O K-XAS on Ag powder at 230 °C in the reaction cell. Spectra (a) and (d) were acquired with a flow of pure O_2 , where (d) was obtained 28 h after spectrum (a). The powder was kept for 24 h under reaction conditions between recording spectra (a) and (d). Spectrum (b) was acquired with a flow of pure Ar 20 min before spectrum (a). Spectrum (e) is the difference between spectra (d) and (c) to remove the contribution of gas phase O_2 from the former. Spectrum (f) presents the (smoothed) difference between spectra (e) and (b) to extract the effect of oxygen loading in Ag. The arrow indicates the x-ray incident energy for the RIXS spectra shown in Fig. 10 were taken.

phase O_2 in the immediate surface vicinity, producing a negative contribution to the TEY-reading. This is rationalized by the fact that the initial Ag film thickness is small compared to the penetration depth of the photons. By contrast, there is no such dip at 531.1 eV in the TFY-mode data. As stated above, the TFY-mode data reflect the entire volume probed by the x-rays and therefore there are only positive contributions from molecular O_2 , marked in a similar way as above.

Figure 9 shows our attempt to separate the gas phase from the solid phase signal in this energy region of XAS by creating a difference spectrum using a reference measurement of gaseous O_2 . The black trace is the difference between O K-XAS spectra recorded in an O_2 gas feed and in an Ar gas feed in immediate succession. With appropriate scaling factors we can retrieve a pure O_2 spectrum that agrees well with other literature. Even the evolution with a pure O_2 gas feed can be followed by creating a difference spectrum, which almost completely cancels the gas phase signal and shows the change of bulk phase oxygen species (turquoise trace).

On the other hand, RIXS is an even more powerful method to project site specific contributions from a single atomic oxygen species. As an example, Figure 10 shows RIXS spectra obtained from the same powder sample as used for obtaining the TFY in Fig. 9, in which the arrow indicates the incident energy of 535 eV used to excite the RIXS spectra. The green trace in Fig. 10 is obtained in a pure O_2 gas feed and the red in a reaction mixture of $C_2H_4:O_2$ (1:2 ratio). The blue difference spectrum shows that a switch to reaction conditions produces a new oxygen species in the Ag powder, which is highlighted by a new peak at 521.3 eV and the rising of a shoulder at 524.8 eV.

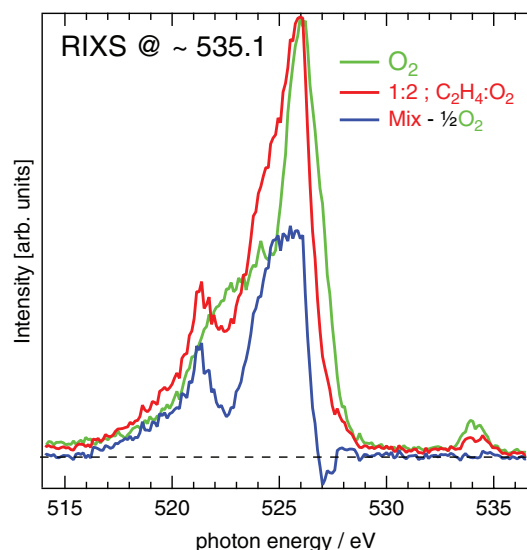


FIG. 10. RIXS measurements of the same Ag power sample as the TFY spectra originates from in Fig. 9. Both the measurement done in pure O_2 and in an oxygen rich reaction mixture were done at $\sim 230^\circ C$.

VII. MODIFICATIONS FOR PHOTOCHEMICAL AND HYDROELECTRO-CATALYSIS

The reaction cell can also be used to perform *in situ* measurements of photochemical- or electrochemical-processes, when applying minor modifications to the basic design layout. We will briefly outline the modifications below.

A. Photochemical *in situ* cell

For photochemical catalysis, e.g., by UV activation, the cell can be used with the thin film sample setup A, where the internal PEEK part is modified so that it may accommodate a LED of appropriate wavelength. Figure 11 shows a cross section of the reaction cell head for such an application.

The main modification over the basic design (Fig. 3) is the embedment of a light emitting diode in the PEEK plug and the insertion of a “sniffer” tube. The sniffer tube (such as a standard Si capillary used in a micro GC) is connected to the vacuum chamber of a mass spectrometer. The flexibility and small total diameter of such a capillary facilitates an easy insertion into the cell exhaust line without undue obstruction. By using a sniffer, the volume of gas to be probed can be chosen more freely, and ultimately allows to increase the portion of reactant gases that can come into contact with the catalyst surface.

B. Electrochemical *in situ* cell

This application for performing electrochemical *in situ* measurements may also be based on the setup A described above.

Fig. 12(a) shows a cross section of the reaction cell head, with the x-ray Si_3N_4 membrane facing to the left. The cell head is largely made in PEEK (orange areas) and all metal parts coming into contact with the liquid is either of pure solid or plated gold, to avoid corrosion products. In (a), a cross sec-

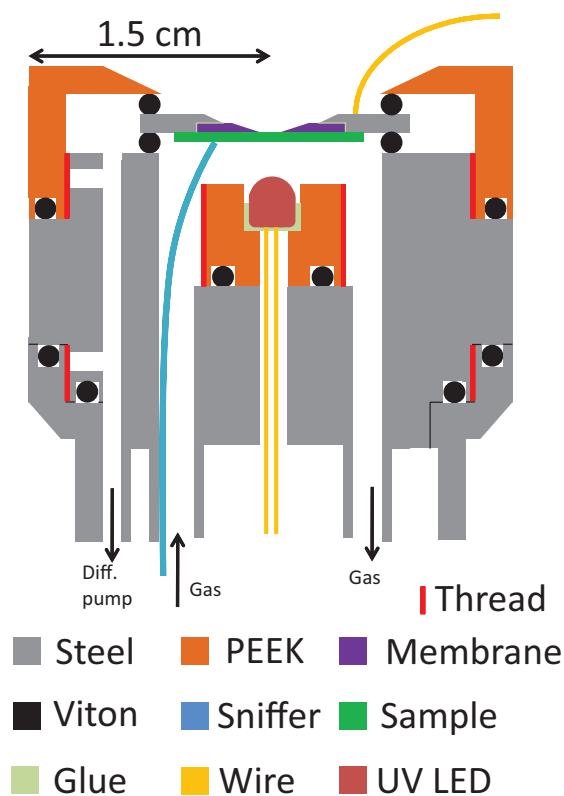


FIG. 11. Thin film setup for *in situ* photochemical measurements, including a sniffer needed at low conversions.

tion is seen with a reference electrode³⁵ inserted at its center, just behind the sample area.

Fig. 12(b) is a face-on view (along the cylindrical axis) of the back part inside the cell. The purple circle symbolizes the electrical contact of the counter electrode. The gray dots are electrical feedthroughs acting as sensors for determining the liquid level in the cell. Liquid can be supplied by a drilled channel that is marked with a filled blue circle at the bottom. This channel is connected via a polymer hose to a syringe that contains a reservoir of the desired liquid. The upper two white circles are drilled channels through which an inert gas may be forced. This gas serves two purposes, namely, (1) to carry reaction products (e.g., H_2 and O_2 if the cell is used for water splitting) to gas analyzers and (2) to allow a change in the liquid level while maintaining a constant pressure inside the cell in order to prevent stress on the membrane. Note that capillary forces between the liquid and the structure surface inside the cell may make it difficult to insure the proper operation of the liquid level sensors. In particular, if there is strong adhesion between the film on the membrane and the liquid vacuum evacuation of the cell could be required.

Fig. 12(c) shows a principle cross section through the working electrode and its holder. The working electrode (sample) is deposited directly onto the membrane using two different masks; one where the connection to the outside is made with a relatively thick film, $+500\text{ nm}$ (and where no material is deposited on the membrane) for electrical contact to a signal wire and one where a thin film is deposited on the mem-

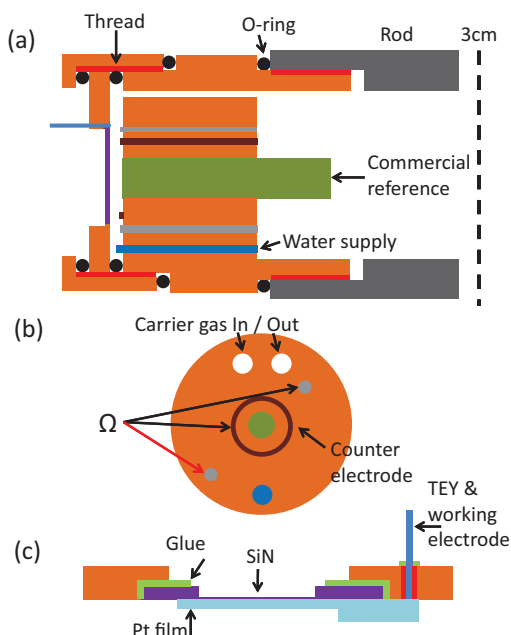


FIG. 12. Film setup for *in situ* electrochemical measurements. (a) cross section of the cell, done in PEEK, screwed on the rod. (b) front side view of the cell, the end facing away from the rod. (c) details of the cell cap containing the membrane and working electrode/sample.

brane and the outside contact. For a Pt film of 25 nm thickness of bulk-Pt density ($21.45 \times 10^3 \text{ kg/m}^3$) the transmission of 530 eV photons (O K-edge) is about 18% at an incidence angle of 45° .³⁶

VIII. CONCLUSIONS

We have designed and constructed a cell suitable for performing heterogeneous catalysis and monitor the chemical reactions *in situ* by synchrotron-radiation-based soft x-ray spectroscopy, i.e., XAS, in both fluorescence yield and electron yield modes, and RIXS by using a commercially available x-ray spectrometer. We have demonstrated the working principle and feasibility by example of ethylene epoxidation over Ag and discussed different approaches for introducing the solid catalytic material and measuring the spectroscopic signals. We have also pointed out how our design may be modified and extended to accommodate *in situ* measurements of photo- or electro-chemical reactions. Thus we present a design for a highly versatile platform for monitoring chemical reactions *in situ* with x-ray spectroscopy.

ACKNOWLEDGMENTS

The authors gratefully acknowledge stimulating discussions with and suggestions from Professor R. Schlögl. We thank the staff at Helmholtz-Zentrum Berlin for providing support for beamtime at U41/PGM BESSY II. This research project has been supported by the European Commission under the 7th Framework Programme through the “Research Infrastructure” action of the “Capacities” Programme, NMI3-II Grant No. 283883. We thank the staff at Advanced

Light Source, ALS, for providing beamtime support. ALS is supported by the Director, Office of Science, Office of Basic Energy Sciences, of the U.S. Department of Energy under Contract No. DE-AC02-05CH11231.

- ¹Recognizing the best in innovation: Breakthrough catalyst, R&D Magazine, p. 20, 2005.
- ²Acmit Market Intelligence, Dechenstr. 17, D-40878 Ratingen, Germany, Market Report: Global Catalyst Market, 2nd ed., January 2009.
- ³V. I. Bukhtiyarov, A. I. Nizovskii, H. Bluhm, M. Hävecker, E. Kleimenov, A. Knop-Gericke, and R. Schlögl, “Combined *in situ* xps and ptrms study of ethylene epoxidation over silver,” *J. Catal.* **238**(2), 260–269 (2006).
- ⁴C. Lamberti, A. Zecchina, E. Groppo, and S. Bordiga, “Probing the surfaces of heterogeneous catalysts by *in situ* ir spectroscopy,” *Chem. Soc. Rev.* **39**, 4951–5001 (2010).
- ⁵B. Hammer, Y. Morikawa, and J. K. Nørskov, “Co chemisorption at metal surfaces and overlayers,” *Phys. Rev. Lett.* **76**, 2141–2144 (1996).
- ⁶E. Kleimenov, H. Bluhm, M. Hävecker, A. Knop-Gericke, A. Pestryakov, D. Teschner, J. A. Lopez-Sanchez, J. K. Bartley, G. J. Hutchings, and R. Schlögl, “XPS investigations of VPO catalysts under reaction conditions,” *Surf. Sci.* **575**(1–2), 181–188 (2005).
- ⁷F. De Groot, “High-resolution x-ray emission and x-ray absorption spectroscopy,” *Chem. Rev.* **101**(6), 1779–1808 (2001).
- ⁸L. J. P. Ament, M. van Veenendaal, T. P. Devereaux, J. P. Hill, and J. van den Brink, “Resonant inelastic x-ray scattering studies of elementary excitations,” *Rev. Mod. Phys.* **83**, 705–767 (2011).
- ⁹J. Forsberg, L.-C. Duda, A. Olsson, T. Schmitt, J. Andersson, J. Nordgren, J. Hedberg, C. Leygraf, T. Aastrup, D. Wallinder, and J.-H. Guo, “System for *in situ* studies of atmospheric corrosion of metal films using soft x-ray spectroscopy and quartz crystal microbalance,” *Rev. Sci. Instrum.* **78**(8), 083110 (2007).
- ¹⁰IARC, Lyon, *IARC Monographs on the Evaluation of Carcinogenic Risks to Humans*, June 2007.
- ¹¹SRI Consulting, 321 Inverness Drive South Englewood, CO 80112, *World Petrochemical on Ethylene Oxide*, January 2009.
- ¹²V. I. Bukhtiyarov and A. Knop-Gericke, “Ethylene epoxidation over silver catalysts,” in *Nanostructured Catalysts: Selective Oxidations* (The Royal Society of Chemistry, 2011), Chap. 9, pp. 214–247.
- ¹³T. C. R. Rocha, A. Oestereich, D. V. Demidov, M. Havecker, S. Zafeiratos, G. Weinberg, V. I. Bukhtiyarov, A. Knop-Gericke, and R. Schlögl, “The silver-oxygen system in catalysis: New insights by near ambient pressure x-ray photoelectron spectroscopy,” *Phys. Chem. Chem. Phys.* **14**, 4554–4564 (2012).
- ¹⁴M. O. Ozbek, I. Onal, and R. A. van Santen, “Why silver is the unique catalyst for ethylene epoxidation,” *J. Catal.* **284**(2), 230–235 (2011).
- ¹⁵R. B. Grant and R. M. Lambert, “A single crystal study of the silver-catalysed selective oxidation and total oxidation of ethylene,” *J. Catal.* **92**(2), 364–375 (1985).
- ¹⁶R. A. Van Santen and H. P. C. E. Kuipers, “The mechanism of ethylene epoxidation,” in *Advances in Catalysis*, edited by Herman Pines, D. D. Eley and Paul B. Weisz (Academic Press, 1987), Vol. **35**, pp. 265–321.
- ¹⁷V. I. Bukhtiyarov, A. I. Boronin, I. P. Prosvirin, and V. I. Savchenko, “Stages in the modification of a silver surface for catalysis of the partial oxidation of ethylene: II. Action of the reaction medium,” *J. Catal.* **150**(2), 268–273 (1994).
- ¹⁸M. A. Banares, “Operando methodology: Combination of *in situ* spectroscopy and simultaneous activity measurements under catalytic reaction conditions,” *Catal. Today* **100**(1–2), 71–77 (2005).
- ¹⁹Ch. Jung, F. Eggenstein, S. Hartlaub, R. Follath, J. S. Schmidt, F. Senf, M. R. Weiss, Th. Zeschke, and W. Gudat, “First results of the soft x-ray micro-focus beamline u41-pgm,” *Nucl. Instrum. Methods Phys. Res. A* **467–468**, Part 1(0), 485–487 (2001).
- ²⁰J. Nordgren, G. Bray, S. Cramm, R. Nyholm, J.-E. Rubensson, and N. Wassdahl, “Soft x-ray emission spectroscopy using monochromatized synchrotron radiation,” *Rev. Sci. Instrum.* **60**(7), 1690–1696 (1989).
- ²¹VG Scientia AB, Vallongatan 1, SE-752 28 Uppsala, Sweden.
- ²²T. Warwick, P. Heimann, D. Mossessian, W. McKinney, and H. Padmore, “Performance of a high resolution, high flux density sgm undulator beamline at the als (invited),” *Rev. Sci. Instrum.* **66**(2), 2037–2040 (1995).

- ²³R. Denecke, P. Väterlein, M. Bässler, N. Wassdahl, S. Butorin, A. Nilsson, J.-E. Rubensson, J. Nordgren, N. Mårtensson, and R. Nyholm, "Beamline i511 at max ii, capabilities and performance," *J. Electron Spectrosc. Relat. Phenom.* **101–103**, 971–977 (1999).
- ²⁴V. I. Bukhtiyarov, "The study of the nature of adsorbed species to build a bridge between surface science and catalysis: Problems of pressure and material gap," *Kinet. Catal.* **44**(3), 420–431 (2003).
- ²⁵*Silson Ltd*, Northampton Road, Blisworth, Northampton, NN7 3DW, England.
- ²⁶*Epoxy Technology, Inc.*, 14 Fortune Drive, Billerica, MA.
- ²⁷B. S. Balzhinimaev, *Kinet Catal.* **40**, 879 (1999).
- ²⁸Chromalox Inc, Cartridge heaters, August 2013.
- ²⁹*Chromalox Ltd*, 2 Purley way, Croydon, Surrey, Cro 3JP, UK.
- ³⁰*X-Ray Data Booklet*, 2nd ed., edited by A. C. Thompson and D. Vaughan (Lawrence Berkeley National Laboratory, University of California, 2001).
- ³¹E. Robert, "Mass spectrometer calibration over wide concentration ranges in multicomponent gas mixtures," *Meas. Sci. Technol.* **21**(2), 025102 (2010).
- ³²P. T. Kristiansen, T. C. R. Rocha, A. Knop-Gericke, J. H. Guo, and L. C. Duda, "In situ soft x-ray spectroscopy of ethylene epoxidation over Ag at 1 atm and 230°C" (unpublished).
- ³³Th. Schedel-Niedrig, R. Schlögl, X. Bao, and M. Muhler, "Surface-embedded oxygen: Electronic structure of ag(111) and cu(poly) oxidized at atmospheric pressure," *Ber. Bunsenges. Phys. Chem.* **101**(7), 994–1006 (1997).
- ³⁴J. Stöhr, *NEXAFS Spectroscopy* (Springer, 1992), Vol. 25.
- ³⁵Gaskatel, *Ag/Agcl Reference Electrode Siref*, August 2013.
- ³⁶B. L. Henke, E. M. Gullikson, and J. C. Davis, "X-ray interactions: Photo-absorption, scattering, transmission, and reflection at $e = 50\text{--}30\,000$ ev, $z = 1\text{--}92$," *At. Data Nucl. Data Tables* **54**(2), 181–342 (1993).